Quantum Well States and Magnetic Coupling between Noble Metals and Ferromagnets (Invited)

G. Mankey – University of Alabama

et al.

Citation of published version:

Ortega, J., et al. (1993): Quantum Well States and Magnetic Coupling between Noble Metals and Ferromagnets (Invited). *Journal of Applied Physics*, 73(10).
DOI: https://doi.org/10.1063/1.353569

Quantum well states and magnetic coupling between noble metals and ferromagnets (invited)

Cite as: Journal of Applied Physics **73**, 5771 (1993); https://doi.org/10.1063/1.353569
Published Online: 04 June 1998

J. E. Ortega, F. J. Himpsel, G. J. Mankey, and R. F. Willis

Quantum well states and magnetic coupling between noble metals and ferromagnets (invited)

J. E. Ortega and F. J. Himpsel
IBM Research Division, Thomas J. Watson Research Center, P.O. Box 218, Yorktown Heights, New York 10598

G. J. Mankey and R. F. Willis
Physics Department, Penn State University, University Park, Philadelphia 16802

We have searched for the electronic states that mediate oscillatory magnetic coupling in superlattices, and have found strong evidence that these are quantum well states, which are created by quantizing the momentum of *s,p*-band states perpendicular to the interfaces. In noble metal layers on ferromagnets we find such states at the Fermi level, where they are able to influence magnetic coupling and transport. They exhibit several traits connecting them with oscillatory magnetic coupling, such as periodicity and spin polarization.

I. INTRODUCTION

The general goal of our work[1–3] is to measure the changes in the electronic structure of magnetic solids as one goes from the bulk to thin films, superlattices, and ultimately to a monolayer. Here, we are specifically addressing the electronic states in multilayers of ferromagnets and noble metals, trying to identify states that give rise to special properties of these structures, such as oscillatory magnetic coupling.[4–18] Noble metal spacer layers are particularly interesting because it is not obvious how a noble metal can transmit magnetic interaction over distances of many atomic layers. In order to narrow the field we notice that states near the Fermi level E_F are expected to contribute the most to magnetic phenomena. After all, the changes in the density of states with kT_c of E_F (T_c=Curie temperature) drive the magnetic phase transition, and states within kT (T=room temperature) are responsible for magnetotransport.

II. QUANTUM WELL STATES

A. Quantization of $k^{\perp}$ in thin films

Electronic states change their character when going from an infinite, periodic solid to a thin film. Figure 1 shows calculations for the electronic states in bulk Ag and for an 11-layer Ag(100) film, using the local density method.[19] In the bulk one has a continuous energy-versus-momentum [$E(k)$] band dispersion, due to the periodic structure of the solid. In a thin film the periodicity perpendicular to the film is broken, and one obtains a set of discrete states along that direction. The number of states per band corresponds to the number of layers in the film. By projecting the energies of the discrete states onto the continuous band dispersion one obtains points that are regularly spaced in the momentum direction perpendicular to the layers, $k^{\perp}$. Thus one may say the momentum has become quantized in the direction perpendicular to the thin film. We often will call these discrete thin-film states quantum well states, even if the presence of a well-shaped potential in the thin film is not obvious.

B. Evidence for discrete thin-film states

To find discrete thin-film states we look at the density of states at fixed parallel momentum ($k^{\parallel}=0$) using inverse photoemission (for empty states) and photoemission (for filled states). Figure 2 shows inverse photoemission spectra[2,3] from Cu films of varying thickness on fcc Fe(100). The latter was in turn grown pseudomorphically on a Cu(100) bulk crystal. As the bulk Cu(100) spectrum on top of Fig. 2 indicates, there is a continuum of states up to about 1.8 eV above E_F, corresponding to a bulk *s,p* band analogous to that shown in Fig. 1 for Ag(100). For thin Cu(100) films the *s,p*-band emission is broken up into several states, which rapidly change their energies with thickness. If we number them from the top down, as in Fig. 1, we notice that they move up in energy with increasing thickness and eventually converge to the band edge at 1.8 eV. This is exactly what we expect from the quantum well states in Fig. 1, since their density increases proportional to the number of layers, such that the states appear to move closer to the band edge with increasing thickness when counted from the top down.

The observation of such discrete states in metals has been rather spotty.[20] This is due to the strict requirements for film smoothness necessary to see them. Figure 3 shows what one is up against. Here the series of rapidly moving peaks is assigned[1] to quantum well states of the *s,p* band of

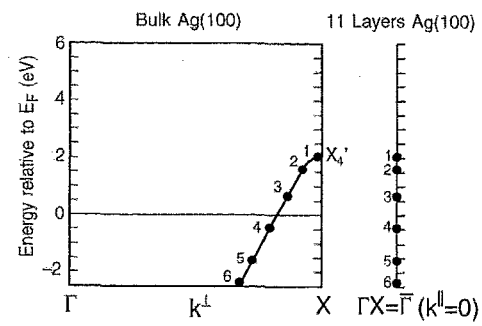

FIG. 1. Discretization of the perpendicular wave vector $k^{\perp}$ in a thin film, demonstrated by comparing band calculations[19] for bulk Ag(100) and for an 11-layer Ag(100) slab.

 0021-8979/93/105771-05$06.00

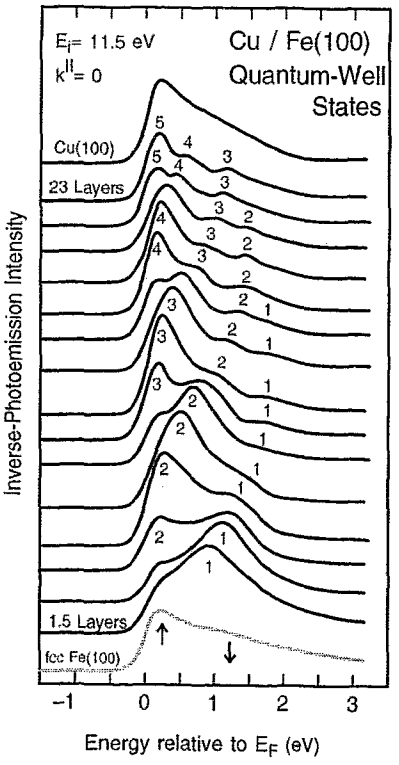

FIG. 2. Thickness dependence of inverse photoemission spectra for Cu films on fcc Fe(100) at $k^{\parallel}=0$. The s,p-band continuum (top) is split up into the numbered quantum well states due to discretization of $k^{\perp}$ in a thin film (see Fig. 1).

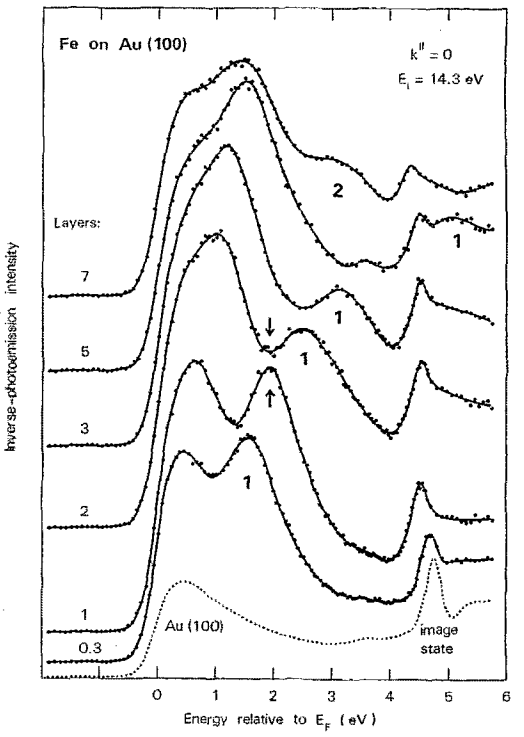

FIG. 3. Quantum well states in the s,p band of bcc Fe films on Au(100), showing the high sensitivity of these states to film smoothness. A maximum turns into a minimum by adding only a single atomic layer (see arrows). Such structures would compensate each other in a rough film.

bcc Fe, grown epitaxially on Au(100). As indicated by the arrows, a peak changes into a valley by adding a single layer of Fe. If the films were not atomically smooth, peaks and valleys from regions with different thickness would average out into a continuum. Indeed, we find that careful electropolishing and cleaning of the substrates is essential for seeing discrete states.

C. Wave function of quantum well states

The simplest way to think about the wave functions in a quantum well is the comparison[1] with an interferometer, e.g., the Fabry–Perot geometry shown in Fig. 4. The two interfaces reflect the electron wave, similar to the mirrors in the optical analog. By moving the interferometer mirrors apart, one creates interference fringes every half wavelength. We can actually observe[1–3] these interference fringes for electrons when changing the film thickness, as shown in Fig. 4. Each interference maximum corresponds to a quantum well state passing through the energy window of our spectrometer. Similar oscillations are seen with photoemission.[3] The wavelength obtained from the spacing between interference maxima is 5.9 ± 0.5 Cu(100) layers, which corresponds to 10.6 Å of Cu. This value is much larger than the Fermi wavelength, which is of atomic dimensions. Thus, a quantum well state seems to contain two types of periodicities in its wave function. This is borne out by a proper theoretical treatment, which shows that we are measuring the wavelength of a slowly varying envelope function that modulates a fast-oscillating Bloch function (Fig. 5).

The framework for discussing thin-film states has been set by extensive work on quantum well states in semiconductors (for a review see Ref. 21). As shown in Fig. 5, the wave function of a quantum well state consists of a rapidly oscillating Bloch function, derived from the bulk states at the nearest band edge, which is modulated by an envelope function. The latter ensures that the boundary conditions are met at the interfaces. The modulation of the Bloch carrier wave with wave vector $k_{\rm edge}$ by the envelope with wave vector $k_{\rm env}$ produces a total wave vector

$$k_{\rm tot}=k_{\rm edge}\pm k_{\rm env}\,. \tag{1a}$$

The total wave vector has to follow the dispersion of a bulk band ($k_{\rm bulk}$), as long as the quantum well is sufficiently wide to neglect changes in bonding near the interfaces. Thus one has a vector diagram for the various wave vectors in the first Brillouin zone, as shown in Fig. 5:

$$k_{\rm bulk}=k_{\rm edge}\pm k_{\rm env}\,. \tag{1b}$$

D. Connection with bulk bands

Using the simple Eq. (1b) it is possible to obtain bulk band dispersions from quantum well states. One simply measures

$$k_{\rm env}=2\pi/\lambda_{\rm env}=\pi/p \tag{2}$$

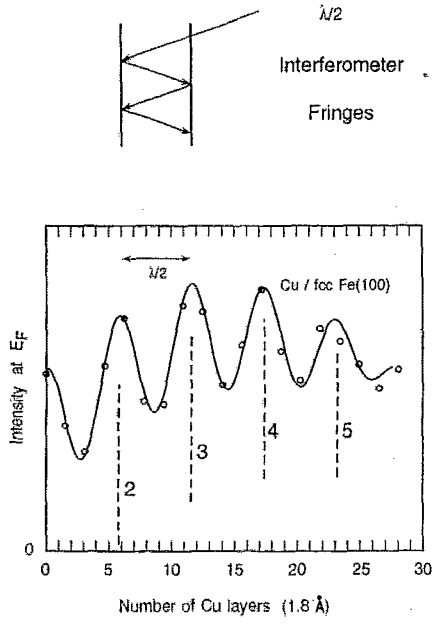

FIG. 4. Oscillations in the inverse photoemission intensity at the Fermi level vs film thickness, shown for the data from Fig. 2. They can be understood either as quantum well states crossing the Fermi level or as interference fringes appearing with a periodicity of half the wavelength λ_{env} of the envelope function (see Fig. 5).

from the periodicity p of intensity oscillations, such as in Fig. 4, and subtracts k_{env} from the wave vector of the band edge. The units work out such that

$$k_{bulk}=1-1/p, \tag{3a}$$

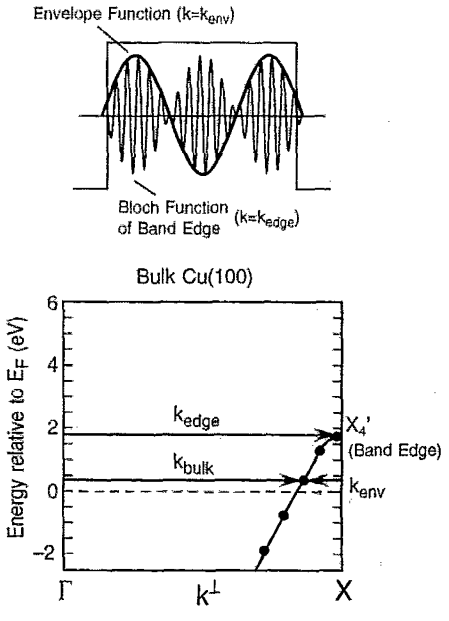

FIG. 5. Model wave function of quantum well states, consisting of a fast-oscillating Bloch function at the band edge that is modulated by a slowly varying envelope function. The corresponding momentum balance shows how the k vector of the envelope function can be obtained from the k vectors of the band edge and a bulk band [Eq. (1)].

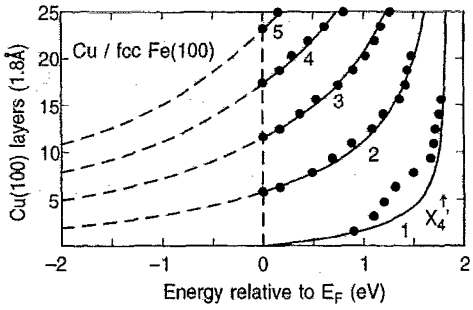

FIG. 6. Plot of the quantum well state features in Fig. 1 (dots) and its theoretical counterpart (lines), which derives quantum well states from bulk bands via Eq. (4). For very thin films (five layers and less) there are deviations due to changes in bonding at the interface atoms.

$$p=1/(1-k_{bulk}), \tag{3b}$$

if k_{bulk} is measured in units of the zone boundary wave vector $k_{ZB}=\pi/d$ (d=layer spacing along the normal) and the period p is measured in monolayers. For the case of the quantum well states at E_F in Cu films (Fig. 4) one has a period of six layers, which corresponds to a Fermi level crossing at 1/6 of ΓX away from the band edge at X, i.e., $k_F/k_{ZB}=0.83$. This is in good agreement with de Haas van Alphen data ($k_F/k_{ZB}=0.827$).

In reverse, it is also possible to predict quantum well states from bulk bands (see Fig. 6 and Ref. 3). The only difference is that we need additional information about the phase of the intensity oscillations, which is not contained in the bulk band structure. It is determined by the sum of the phase shifts for the reflections at the two interfaces, which in turn is determined by the (complex) band structure of the two layers confining a quantum well. We obtain a formula for the thickness-versus-energy relation of the nth quantum well state, $d_n(E)$ by adding $(n-1)$ times the period p [from Eq. (3b)] to the thickness for the first state, which is given by a fraction ϕ of the period, with ϕ being the sum of the phase shifts for the reflections at the two interfaces, measured in units of 2π:

$$d_n(E)=[n-1+\phi\,(E)]/[1-k_{bulk}(E)]. \tag{4}$$

Thereby d_n is given in monolayers, and k_{bulk} in units of the zone boundary wave vector k_{ZB} at X. For Fig. 6 we use an empirical band structure $k_{bulk}(E)$. The phase shift $\phi(E)$ is found by matching the calculated structure plot (see lines in Fig. 6) to the data points for one of the quantum well states. Then all the other quantum well states are completely determined.

The simple picture of quantum well states as bulk states, discretized by the finite slab thickness, is expected to break down when going towards the monolayer limit. The atoms in the quantum well will feel their foreign neighbors across the interface and will change their bulk-like bonding. The onset of this effect can be observed by comparing our data with the predictions of the bulk-like quantum well model in the low thickness limit. Looking at the structure plot in Fig. 6 we notice that the $n=1$ quantum well state deviates systematically from the energy predicted by the

bulk-like quantum well model (lines), starting at a thickness of about five layers. This indicates that not only the interface atoms, but also their neighbors are affected.

III. QUANTUM WELL STATES AND OSCILLATORY MAGNETIC COUPLING

An oscillatory magnetic coupling has been observed in superlattices consisting of alternating layers of ferromagnets and noble metals.[4–12] This effect has potential for applications in magnetic storage since it gives rise to a large (giant) magnetoresistance effect at reasonably low switching fields that can be used in reading magnetically stored data. Our thin-film studies serve as model for more complex structures by representing one period of a superlattice or a spin valve.[13] A single layer is expected to simulate a superlattice rather well, since the observed magnetic coupling depends mainly on the thickness of the noble metal spacer layers, and little on the thickness of the ferromagnetic layers. This jibes well with our observation that quantum well states are absent at the Fermi level in ferromagnets (although they are seen a few eV above E_F, as shown in Fig. 3). Therefore, simulating a thin magnetic film by an infinitely thick, ferromagnetic substrate does not affect the magnetic coupling through the noble metal.

There are several strong indications that the quantum well states observed at the Fermi level in thin noble metal films are in fact the carriers of the magnetic coupling: They appear with a period equal to the magnetic period in cases where a comparison can be made, e.g., for fcc Cu/Co(100). They also are found to be spin polarized despite their *s,p* character, e.g., for Ag/Fe(100) thus providing a magnetic interaction. Other noteworthy consistency checks come from the prediction that the magnetic coupling period should depend only on the noble metal spacer, not on the ferromagnet, while the phase depends purely on the ferromagnet. In the following we will explain these phenomena using the quantum well state picture developed in Sec. II. It turns out that the result for the periodicity of the magnetic coupling is identical to that obtained from Rudermann–Kittel–Kasuya–Yosida (RKKY) theory, when evaluated at discrete lattice spacings.[14–18] Thus we have found a real-space picture that might make the workings of the RKKY formalism more tractable.

A. Spin polarization of quantum well states

First we focus on the spin polarization of quantum well states. As an example we discuss fcc Ag(100) on bcc Fe(100), which has also been studied with spin-polarized photoemission.[22] An occupied minority spin state was found in Ref. 22 (open circles in Fig. 7), which connects with our $n=2$ quantum well state through the Fermi level. Thus we have good reason to believe that the quantum well state has minority spin character as well. This can be explained from the band structures for Ag(100) and Fe(100) in Fig. 8 (see Refs. 19, 23). The minority spin Δ_1 bands exhibit a gap at E_F in Fe(100), allowing the formation of true quantum well states in the minority Δ_1 *s,p* band of Ag(100). The majority spin Δ_1 states of Ag(100), on the other hand, couple to the majority Δ_1 band of Fe(100) at the Fermi level, and form a continuum of Bloch states, instead of discrete quantum well states.

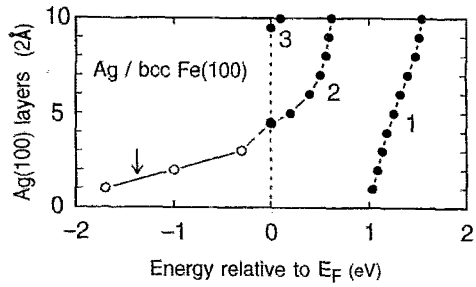

FIG. 7. Structure plot analogous to Fig. 6 of quantum well states for Ag on bcc Fe (100). Spin-polarized photoemission data (open circles, see Ref. 22) show that the $n=2$ state is spin polarized, and thus able to transmit magnetic coupling through the noble metal.

B. Oscillation period

The periodicity in the appearance of quantum well states at the Fermi level E_F can be traced directly to the Fermi wave vector k_F by using Eq. (3b). Indeed, we find that the de Haas van Alphen Fermi wave vectors of $0.827k_{ZB}$ for Cu and $0.819k_{ZB}$ for Ag give rise to periods of $1/(1-0.827)=5.8$ layers for Cu and $1/(1-0.819)=5.5$ layers for Ag, which agree with our measured quantum well state periods of 5.9 layers for Cu/Co(100) and 5 layers for Ag/Fe(100) within the experimental accuracy. In this context it should be mentioned that an accurate film thickness calibration is not easy for such thin films. We have used high-resolution Rutherford backscattering[24] for the inverse photoemission data and reflection high-energy electron diffraction (RHEED) oscillations for the photoemission data, in addition to monitoring by a quartz oscillator. The oscillation periods from inverse photoemission and photoemission agreed within 5%.

The magnetic oscillation periods reported[5–9] for Cu/Co(100) and Cu/Fe(100) in the fcc phase are also about

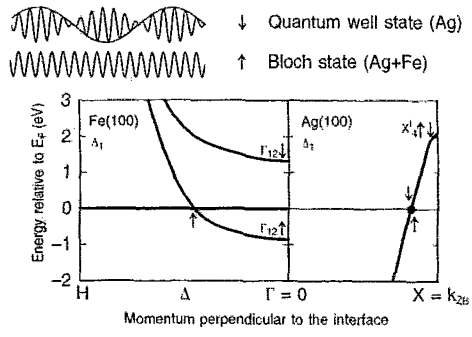

FIG. 8. Explanation of the minority spin character of the quantum well states for Ag/Fe(100) in Fig. 7. The absence of Δ_1 minority spin states at the Fermi level in Fe(100) produces minority spin quantum well states in the Ag(100) film. The majority spin states in Ag(100), however, hybridize with the majority spin states in Fe(100) and form a continuum of bulk-like bands.

6 layers. An additional, shorter period of 2.6 layers has been reported on one occasion.[7] Both periods are expected from RKKY theory,[17] the long one from states at $k^{\parallel}=0$, the short one from states at large $k^{\parallel}$. In our quantum well state picture we have the same physics, with quantum well states at $k^{\parallel}=0$ giving the long period, and quantum well states at large $k^{\parallel}$ the short period.[3] The latter are not detected in our measurement geometry, which is restricted to $k^{\parallel}=0$. It would be interesting to look in the proper region of k space for quantum well states responsible for the short period.

Recent magnetic measurements on the Ag/Fe(100) system[25,26] indicate equally as good an agreement with the quantum well state oscillations as for Cu/Co(100) and Cu/Fe(100). Again, there is a long period (5.7 layers) and a short period (2.4 layers),[26] with the long period corresponding to the quantum well state oscillations at $k^{\parallel}=0$. The situation is the same as for Cu(100) spacers, since the Fermi surfaces of Cu and Ag are similar near the [100] direction.

C. Oscillation phase

The phase of the quantum well state oscillations is given by the phase shifts encountered by the wave function as it is back-reflected at the boundaries of the quantum well.[27] Thus it depends on the band structure of the medium that confines the quantum well states and on the structure of the interfaces. In magnetic superlattices we have the ferromagnet as the medium that confines the quantum well states to the noble metal spacer layer. In our experiments there is vacuum on one side and the ferromagnet on the other. Therefore, the oscillation phase seen in our experiments is generally not representative of the phase of magnetic oscillations in a superlattice.

Comparing period and phase of the magnetic oscillations with experiment we expect to obtain orthogonal insights: The period should be a bulk property of the noble metal spacer layer, while the phase should depend on the band structure of the ferromagnet and on the interface. While it is too early to draw definitive results from the available data due to structural uncertainties, there seem to be indications that in the case of Cu/Co(100) vs Cu/Fe(100) one sees indeed comparable periods, but a variety of phases.[5-9]

[1] F. J. Himpsel, Phys. Rev. B **44**, 5966 (1991).
[2] J. E. Ortega and F. J. Himpsel, Phys. Rev. Lett. **69**, 844 (1992).
[3] J. E. Ortega, F. J. Himpsel, G. J. Mankey, and R. F. Willis, Phys. Rev. B **47**, 1540 (1993).
[4] S. S. P. Parkin, N. More, and K. P. Roche, Phys. Rev. Lett. **64**, 2304 (1990); S. S. P. Parkin, R. Bhadra, and K. P. Roche, *ibid.* **66**, 2152 (1991); S. S. P. Parkin, *ibid.* **67**, 3598 (1991).
[5] J. J. de Miguel, A. Cebollada, J. M. Gallego, R. Miranda, C. M. Schneider, P. Schuster, and J. Kirschner, J. Magn. Magn. Mater. **93**, 1 (1991).
[6] Z. Q. Qiu, J. Pearson, and S. D. Bader, Phys. Rev. B **46**, 8659 (1992).
[7] M. T. Johnson, S. T. Purcell, N. W. E. McGee, R. Coehoorn, J. aan de Stegge, and V. Hoving, Phys. Rev. Lett. **68**, 2688 (1992).
[8] F. Petroff, A. Barthélemy, D. H. Mosca, D. K. Lottis, A. Fert, P. A. Schroeder, W. P. Pratt, Jr., and R. Loloee, Phys. Rev. B **44**, 5355 (1991).
[9] W. R. Bennett, W. Schwarzacher, and W. F. Egelhoff, Phys. Rev. Lett. **65**, 3169 (1990).
[10] Z. Celinski and B. Heinrich, J. Magn. Magn. Mater. **99**, L25 (1991).
[11] A. Fuβ, S. Demokritow, P. Grünberg, and W. Zinn, J. Magn. Magn. Mater. **103**, L221 (1992).
[12] J. Unguris, R. J. Celotta, and D. T. Pierce, Phys. Rev. Lett. **67**, 140 (1991); *ibid.* **69**, 1125 (1992).
[13] B. Dieny, V. S. Speriosu, S. Metin, S. S. P. Parkin, B. A. Gurney, P. Baumgart, and D. R. Wilhoit, J. Appl. Phys. **69**, 4774 (1991).
[14] D. M. Edwards, J. Mathon, R. B. Muniz, and M. S. Phan, Phys. Rev. Lett. **67**, 493 (1991).
[15] D. M. Deaven, D. S. Rokhsar, and M. Johnson, Phys. Rev. B **44**, 5977 (1991); *ibid.* **69**, 1125 (1992).
[16] F. Herman, J. Sticht, and M. Van Schilfgaarde, J. Appl. Phys. **69**, 4783 (1991); F. Herman and R. Schrieffer, Phys. Rev. B **46**, 5806 (1992).
[17] P. Bruno and C. Chappert, Phys. Rev. Lett. **67**, 1602 (1991); **67**, 2592 (1991); Phys. Rev. B **46**, 261 (1992).
[18] R. Coehoorn, Phys. Rev. B **44**, 9331 (1991).
[19] For bulk Ag, see H. Eckardt, L. Fritsche, and J. Noffke, J. Phys. F **14**, 97 (1984). For the Ag(100) slab calculation, see H. Erschbaumer, A. J. Freeman, C. L. Fu, and R. Podloucky, Surf. Sci. **243**, 317 (1991). In Fig. 1 this calculation has been shifted up by 0.5 eV to match the X_4' point of the bulk calculation.
[20] R. E. Thomas, J. Appl. Phys. **41**, 5330 (1970); R. C. Jaklevic and John Lambe, Phys. Rev. B **12**, 4146 (1975); H. Iwasaki, B. T. Jonker, and Robert L. Park, Phys. Rev. B **32**, 643 (1985); S. Å Lindgren and L. Walldén, Phys. Rev. Lett. **61**, 2894 (1988); T. Miller, A. Samsavar, G. E. Franklin, and T.-C. Chiang, *ibid.* **61**, 1404 (1988).
[21] G. Bastard, *Wave Mechanics Applied to Semiconductor Heterostructures* (Les Editions de Physique, Les Ulis, France, 1988), Chap. III.
[22] N. B. Brookes, Y. Chang, and P. D. Johnson, Phys. Rev. Lett. **67**, 354 (1991).
[23] The bands shown in Fig. 6 for Fe are from J. Callaway and C. S. Wang, Phys. Rev. B **16**, 2095 (1977). For experimental results, see A. Santoni and F. J. Himpsel, Phys. Rev. B **43**, 1305 (1991).
[24] We would like to acknowledge M. Copel for the Rutherford backscattering calibration of our film thicknesses.
[25] Z. Celinski, B. Heinrich, and J. F. Cochran (these proceedings).
[26] J. Unguris, R. J. Celotta, and D. T. Pierce (these proceedings).
[27] P. M. Echenique and J. B. Pendry, Prog. Surf. Sci. **32**, 111 (1990).